Sources of artefacts in the electrospray ionization mass spectra of saturated diacylglycerophosphocholines: From condensed phase hydrolysis reactions through to gas phase interclus...

ARTICLE *in* JOURNAL OF THE AMERICAN SOCIETY FOR MASS SPECTROMETRY · MARCH 2006

Impact Factor: 2.95 · DOI: 10.1016/j.jasms.2005.11.009 · Source: PubMed

Sources of Artefacts in the Electrospray Ionization Mass Spectra of Saturated Diacylglycerophosphocholines: From Condensed Phase Hydrolysis Reactions Through to Gas Phase Intercluster Reactions

Patrick F. James* and Matthew A. Perugini

Department of Biochemistry and Molecular Biology, Bio21 Molecular Science and Biotechnology Institute, The University of Melbourne, Victoria, Australia

Richard A. J. O'Hair

School of Chemistry, Bio21 Molecular Science and Biotechnology Institute, The University of Melbourne, Victoria, Australia

The mass spectra of diacylglycerophosphocholine phospholipids comprised of saturated fatty acids (1,2-dipentanoyl-sn-glycero-3-phosphocholine (D5PC); 1,2-dihexanoyl-sn-glycero-3-phosphocholine (D6PC), and 1,2-dimyristoyl-sn-glycero-3-phosphocholine (D14PC)) are sensitive to the electrospray ionization (ESI) conditions. When fresh solutions of phospholipid in 10 mM ammonium acetate are subjected to ESI, protonated oligomeric clusters, $[DxPC_n + H]^+$ (x = 5, 6, and 14) are observed in the following different types of mass spectrometers: 3D-quadrupole ion trap; linear ion trap, and triple quadrupole. The formation of the protonated cluster ions is not unique to the ion trap instruments, although they tend to be more abundant in these instruments. As the ESI solutions age, new ions are observed, which correspond to acid-catalyzed solution phase deacylation reactions. The collision induced dissociation fragmentation reactions of the oligomer cluster ions exhibit a distinct dependence on the cluster size, with the larger clusters ($n > 2$) simply fragmenting via the loss of lipid monomers. In contrast, the fragmentation of the dimeric cluster ion is unique, resulting in a number of additional reactions including covalent bond formation via intermolecular cluster S_N2 reactions and S_N2 transfer of a methyl group. The nature of the charge has a significant role in the formation of products via these intermolecular cluster reactions. Changing the head group to phosphoethanolamine "switches off" the S_N2 reactions, while changing the cation from a proton to either a sodium or a potassium ion, diminishes the intermolecular reactions relative to monomer loss. Semi empirical PM3 calculations on $[D6PC_2 + H]^+$ suggest that the S_N2 reactions are thermodynamically favored over simple monomer loss. These results have important implications in the field of lipidomics. (J Am Soc Mass Spectrom 2006, 17, 384–394)

Electrospray ionization tandem mass spectrometry (ESI/MS/MS) has opened up new opportunities to study the gas-phase chemistry of noncovalent complexes and salts, including those of biological relevance. While many simple protonated dimer clusters simply fragment via monomer formation [1], there are an ever-increasing number of examples where covalent bond formation between the two monomers accompanies fragmentation. For example, noncovalent complexes of phosphate anions of biological interest undergo condensation reactions including: diphosphate formation [2], triphosphate formation [3], and phosphorylation of peptides [4]. Noncovalent complexes between nucleobases and sugars promote the cleavage of saccharide bonds via condensation reactions [5]. Furthermore, a number of tetralkylammonium salts undergo gas-phase S_N2 reactions, including those involving organic counter ions (eq 1a) [6, 7], inorganic counter ions (eq 2) [8], counter ions derived from biomolecules such as peptides (eq 3a, b) [9], DNA (eq 4a) [10], and glycerophosphocholine adducts (eq 5) [11]. For larger alkyl groups, these S_N2 reactions are often in competition with E2 reactions (eqs 1b, 3c, and 4b).

Published online January 27, 2006

This article is Part 48 of the series "Gas Phase Ion Chemistry of Biomolecules."

Address reprint requests to Associate Professor R. A. J. O'Hair, School of Chemistry, Bio21 Molecular Science and Biotechnology Institute, The University of Melbourne, Parkville, Victoria 3010, Australia. E-mail: rohair@unimelb.edu.au

* Also at the School of Chemistry, Bio21 Molecular Science and Biotechnology Institute, The University of Melbourne, Victoria, Australia.

1044-0305/06/$32.00
doi:10.1016/j.jasms.2005.11.009

Received July 1, 2005
Revised November 17, 2005
Accepted November 17, 2005

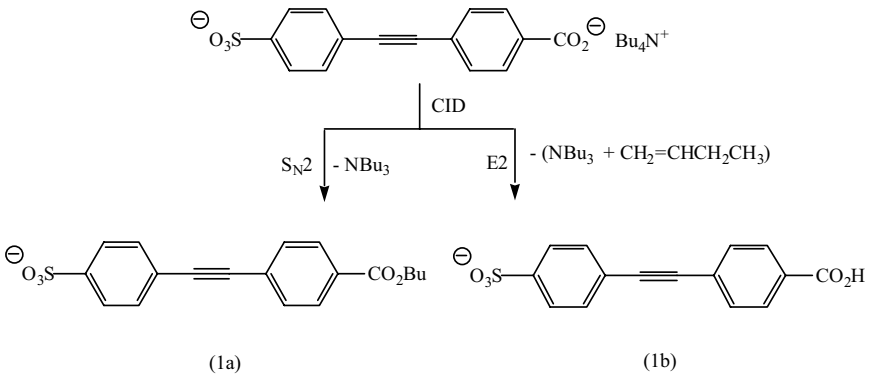

$$[Mo_2O_7]^{2-}\,Bu_4N^+ \xrightarrow[-\,NBu_3]{CID} [Mo_2O_6(OBu)]^- \quad (2)$$

$$[Peptide\text{-}2H]^{2-}\,Me_3NCH(Me)Ph^+ \xrightarrow{CID} \begin{cases} [Peptide\text{-}2H{+}Me]^- + Me_2NCH(Me)Ph & (3a) \\ [Peptide\text{-}2H{+}CH(Me)Ph]^- + Me_3N & (3b) \\ [Peptide\text{-}H]^- + CH_2{=}CHPh + Me_3N & (3c) \end{cases}$$

$$[dCCGG\text{-}2H]^{2-}\,Bu_4N^+ \xrightarrow{CID} \begin{cases} [dCCGG\text{-}2H{+}Bu]^- + NBu_3 & (4a) \\ [dCCGG\text{-}H]^- + NBu_3 + CH_2{=}CHCH_2CH_3 & (4b) \end{cases}$$

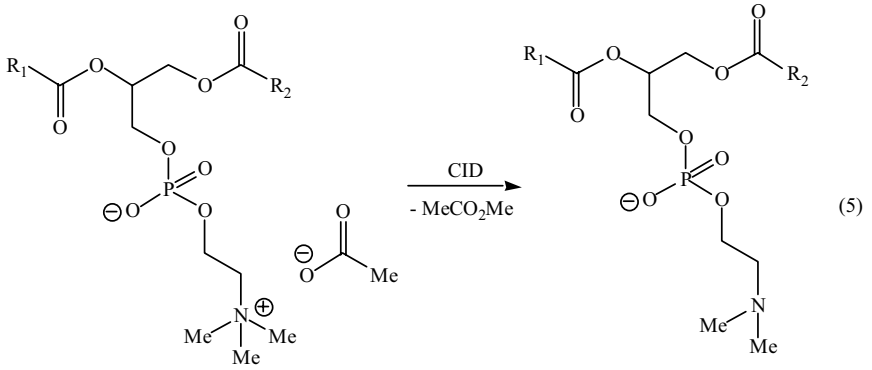

As part of an ongoing investigation into protein–protein, protein–lipid, and lipid–lipid interactions of lipoprotein constituents [12], we were interested in employing ESI/MS/MS to examine the association reactions of the simple saturated diacylglycerophosphocholines shown in Scheme **1**. Previous studies by Hanson et al. [13] have shown that such species form a distribution of gas-phase proton bound oligomers ("micelles" [14]). When special collisional cooling conditions were used, higher oligomers could be formed for D14PC, (3 in Scheme **1**), with the largest complex being assigned to 95 lipid molecules with a charge state of +12 and a mass of 64,410 Da. Thus, we were intrigued at examining the gas-phase fragmentation of these oligomeric species under CID MS/MS conditions. Here we report: (1) on the formation of oligomeric species and other artefacts under ESI/MS conditions; (2) that the fragmentation of the dimer cluster cations are unique, resulting in a number of reactions including covalent bond formation via intermolecular cluster S_N2 reactions. Given the intense interest in lipid profiling via ESI/MS/MS [15], these

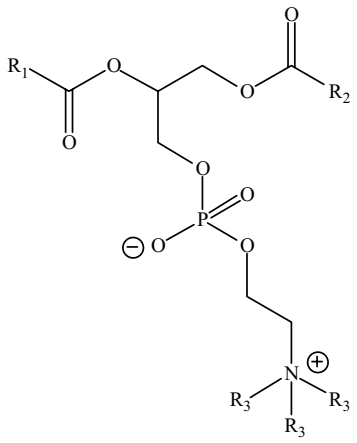

(1) D5PC: $R_1 = R_2 = (CH_2)_3CH_3$; $R_3 = CH_3$

(2) D6PC: $R_1 = R_2 = (CH_2)_4CH_3$; $R_3 = CH_3$

(3) D14PC: $R_1 = R_2 = (CH_2)_{12}CH_3$; $R_3 = CH_3$

(4) D6PE: $R_1 = R_2 = (CH_2)_4CH_3$; $R_3 = H$

Scheme 1

results may have important implications in the generation of artefacts via solution phase reactions or gas-phase intermolecular cluster reactions.

Experimental

Materials

The following lipid samples were obtained from Avanti Polar Lipids (Alabaster, AL) and used without further purification: 1,2-dipentanoyl-sn-glycero-3-phosphocholine (D5PC in Scheme **1**); 1, 2-dihexanoyl-sn-glycero-3-phosphocholine (D6PC in Scheme **1**); 1, 2-dimyristoyl-sn-glycero-3-phosphocholine (D14PC in Scheme **1**); and 1, 2-dihexanoyl-sn-glycero-3-phosphoethanolamine (D6PE in Scheme **1**). All other chemicals were obtained from Sigma-Aldrich (Sydney, Australia) and used as received.

Quadrupole Ion Trap Mass Spectrometry Experiments

The most extensive series of experiments were performed using commercially available quadrupole ion trap mass spectrometers (Finnigan-MAT LCQ classic and DECA, San Jose, CA) equipped with electrospray ionization (ESI). The concentrations of the D5PC and D6PC ESI solutions were 8 mM, which corresponds to sub-micellar concentrations of these phospholipids, given that their critical micellar concentrations (CMCs) are: 85–105 mM for D5PC [16a] and 10–16 mM for D6PC [16]. The concentration of D14PC employed in this study was 2.5 mM. Both short-chain phospholipids were sprayed in 10 mM ammonium acetate at pH 6.1, whereas DMPC was initially diluted 1:10 in acetonitrile/10 mM ammonium acetate from a stock of 25 mM before analysis. The sodiated and potassiated clusters were formed by adding NaCl and KCl to the lipid solutions to a final concentration of 40 mM. Since phosphocholine (PC) was available as its calcium salt, and ESI/MS of this salt mainly produces calcium containing cluster ions, we used the well known calcium chelator, ethylenediaminetetraacetic acid (EDTA) to replace the Ca^{2+} with H^+. Thus to form mixed phosphocholine (PC)-D6PC cluster ions, a solution of 4 mM D6PC, 4 mM PC (Ca^{2+} salt), and 4 mM EDTA in 10 mM NH_4OAc, pH 6.1 was prepared. The samples were introduced into the mass spectrometer via electrospray ionization using a flow rate of 3.0 μL/min. Typical ESI source conditions used were: spray voltage, 5.0 kV, capillary temperature, 200 °C, nitrogen sheath pressure, 60 psi, and capillary voltage/tube lens offset, 0 V. The injection time was set at 5 ms for initial scans and was subsequently manually optimized to obtain best signal (but never higher than 100 ms). Collision-induced dissociation (CID) was carried out by mass selecting the desired ions with a 3–5 Th window, and subjecting them to the following typical conditions: activation energy between 16 and 20%; activation (Q), 0.25 V, and activation time 100 ms.

Linear Ion Trap- Fourier Transform Ion-Cyclotron Resonance Mass Spectrometry Experiments

Key high-resolution mass spectrometry experiments were carried out using an 8 mM solution of D6PC on a Finnigan-MAT LTQ-FTMS instrument equipped with electrospray ionization (ESI). The sodiated and potassiated clusters were formed by adding NaCl and KCl to the lipid solutions to a final concentration of 40 mM. The samples were introduced to the mass spectrometer via electrospray ionization using a flow rate of 3.0 μL/min. Typical ESI source conditions used were: spray voltage, 5.0 kV, capillary temperature, 200 °C, nitrogen sheath pressure, 40 psi, and capillary voltage/tube lens offset, 0 V. The injection time was set using the AGC function. CID was carried out by mass selecting the desired ions with a 3 Th window and subjecting them to the following typical conditions: activation energy between 16 and 20%; activation (Q), 0.25 V, and activation time 100 ms for analysis in the ion trap. For high-resolution mass spectrometry experiments, the analyte was transferred to the FTMS cell. Similar CID conditions were used, except that the activation energy was raised by 10%. To overcome the time of flight effect, CID spectra containing low mass ions that were lost during the transfer to the FTMS cell were analyzed by changing the mass window of ions transferred.

Triple Quadrupole Mass Spectrometry Experiments

ESI/MS and tandem mass spectrometry experiments were carried out on a Micromass Quattro II triple quadrupole mass spectrometer (Micromass Ltd., Manchester, UK) equipped with electrospray ionization. The concentration of D6PC was 2 mM in solution (10 mM ammonium acetate, pH 6.1). The samples were introduced into the mass spectrometer via electrospray ionization using a flow rate of 3 μL/min. Typical ESI source conditions used were: spray voltage, 3.5 kV, HV lens, 0.6 kV, skimmer offset, 5 V, skimmer, 1.5 V, RF lens, 0.2 V and source temperature 80 °C. In-source CID was carried out by varying the cone voltage between 10 and 150 V, as displayed on spectra in the supplementary material section (which can be found in the electronic version of this article).

Results and Discussion

Formation of Cluster Ions of Diacylglycerophosphocholines as Well as Other Artefacts Under ESI/MS Conditions

ESI/MS of diacylglycerophosphocholines, DxPC (x = 5, 6, and 14), in the positive ion mode yields a range of protonated oligomers $[DxPC_n + H]^+$. Due to the limited mass range of the quadrupole ion trap (4000 Th) and the lack of specialized collisional cooling conditions, the oligomers with the largest number of monomer units that we have been able to detect are $[D6PC_8 + H]^+$ and $[D6PC_{15} + 2H]^{2+}$. In addition, using different mass spectrometers, we have shown that these gas-phase cluster ions can be formed with different types of ESI sources and mass analyzer (although the relative abundances of the cluster ions are higher in the LCQ). This suggests that the interactions observed in the gas phase maybe similar to those present in the solution phase. Moreover, the concentration of D6PC at which these protonated cluster ions are detectable can be as low as 80 μM in the LCQ, with the monomer detectable at a tenfold lower concentration of 8 μM (Supplementary Material Figure S1, which can be found in the online version of this article).

In conjunction with the cluster ions observed in the ESI/MS, we also found ions at *m/z* 98 less than the respective cluster ion peaks in both the LCQ and triple quadrupole ESI/MS (Supplementary Material Figure S2). These ions were observed for samples that had been stored for a month at 4 °C or for 48 h at room temperature (Supplementary Material Figure S2) and could arise from acid-hydrolysis of an ester bond in the glycerol backbone of D6PC, leaving the glycerol moiety with a single ester bond to the phosphocholine head group. The exact mass difference was determined by LTQ-FTMS to be 98.0610 Da, which agrees with the theoretical mass of the 6 carbon fatty acid ($C_6H_{10}O$, 98.0726 Da). Deacylation reactions, while apparently not reported in the ESI/MS literature of phospholipids, have been reported for acid-treated phospholipid preparations [17].

ESI/MS/MS of Proton Bound Homo- and Hetero-Oligomers of Diacylglycerophosphocholines

Given the significant recent interest of the fragmentation behavior of multicomponent noncovalent complexes under CID conditions [18], we wanted to examine the behavior of proton bound homo- and hetero-oligomers of D5PC (1), D6PC (2), and D14PC (3). Due to the limited mass range of the quadrupole ion trap, the oligomers with the largest number of monomer units that we have been able to examine under CID conditions are $[DnPC_4 + H]^+$ (for n = 5 and 6) and $[D14PC_3 + H]^+$. A total of 36 product ion spectra of cationized homo- and hetero-oligomers were examined. The tandem mass spectra of the $[D6PC_n + H]^+$ series of homo-oligomers (n = 1–4) are shown in Figure 1, and are representative of all other proton bound homo-oligomers.

All the proton bound homo-oligomers $[D6PC_n + H]^+$ simply fragment via loss of a monomer unit when n > 2. Fragmentation of the protonated dimer, however, is unique and results not only in the loss of a zwitterionic monomer, but also in covalent bond formation via intermolecular cluster S_N2 reactions as well as other competing reactions. These intermolecular cluster reactions are not unique to the D6PC homo-dimers, and were also observed in the LCQ tandem mass spectra of the D5PC and D14PC homo-dimers (Table 1), as well as the $[D5PC + H + D6PC]^+$, $[D5PC + H + D14PC]^+$, and $[D6PC + H + D14PC]^+$ hetero-dimers (Supplementary Material Figure S3).

In the case of $[D6PC_2 + H]^+$, four main types of ions are observed (Figure 1c): (1) loss of a monomer to give the $[D6PC + H]^+$ ion at *m/z* 454; (2) formation of a product ion at *m/z* 637; (3) an intermolecular cluster S_N2 reaction with expulsion of trimethylamine to give a $[D6PC_2 + H - Me_3N]^+$ product ion at *m/z* 848; and (4) an intermolecular cluster S_N2 methylation reaction to give a $[D6PC + Me]^+$ product ion at *m/z* 468. This gives rise to the following questions: What types of mechanisms might yield the key product ions at *m/z* 468, at *m/z* 848, and at *m/z* 637? How do these mechanisms dictate the structure of these product ions? It seems likely that each of these intercluster reactions are triggered by the anionic phosphate oxygen, which can potentially initiate the different mechanisms shown as (a) to (e) in Schemes **2**, **3**, and **4**.

The product ion at *m/z* 468 arises from S_N2 methylation Reaction (a) shown in Scheme **2**. This reaction is directly related to the S_N2 reactions in salts discussed in the introduction (eqs 2, 3a, 3b, and 4a). The only difference is the overall charge for each of the systems, the nature of the amine leaving groups and the anionic nucleophiles.

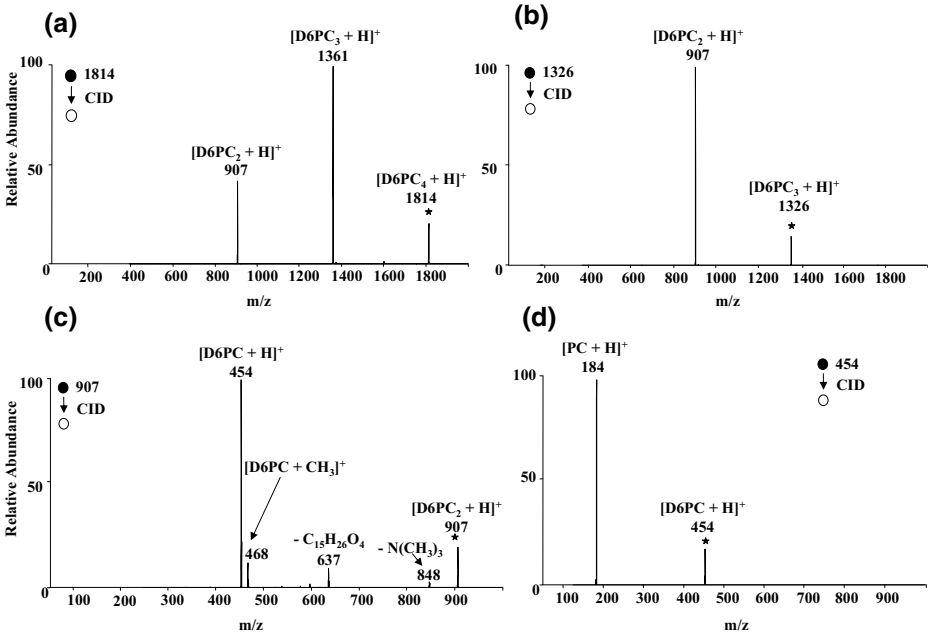

Figure 1. LCQ CID MS/MS of (**a**) $[D6PC_4 + H]^+$; (**b**) $[D6PC_3 + H]^+$; (**c**) $[D6PC_2 + H]^+$; (**d**) $[D6PC + H]^+$. The mass selected precursor ion is designated by an asterisk.

The product ion at *m/z* 848 arises from Me_3N loss. There are two possible mechanisms for this loss. The first, (Reaction (b) of Scheme **3**), involves attack of the phosphate oxy anion onto the neighboring head group in a similar fashion to the S_N2 methylation (Reaction (a) in Scheme **2**). Thus the only difference between these intermolecular S_N2 reactions is the nature of the carbon attacked and the resulting leaving group. An important consequence of the mechanism shown in Path (b) is that it results in a "cross-linked" $[D6PC_2 + H - Me_3N]^+$ product. In contrast, if Me_3N loss occurs via an intramolecular mechanism as shown in Path (c) of Scheme **3**, the $[D6PC_2 + H - Me_3N]^+$ product is a noncovalent complex. Thus, these different pathways give rise to two structural distinct product ions, which should be distinguishable from each other by further CID reactions. The results of such studies are discussed in detail in another section below.

The ion at *m/z* 637 could also arise from either of two pathways, depending on whether the phosphate oxy anion attacks in an intermolecular (Scheme **4**, Path (d) or intramolecular (Scheme **4**, Path (e) fashion. Unfortunately, both mechanisms yield the same products and are thus not readily distinguished. Interestingly, the ionic product corresponds to the $[D6PC + PC + H]^+$ heterodimer. The intermolecular elimination mechanism seems unlikely because the protons on the glycerol backbone are less acidic than the α-protons on the fatty acid side chains and, thus, loss of the fatty acid moiety as ketene would be expected to dominate any intermolecular elimination reaction [19]. In contrast, the in-

Table 1. LCQ product ion spectra of the cationized homo-dimers $[DnPC_2 + X]^+$ (where n = 5, 6 and 14 acyl chain length and X = H, Na or K)

		Fragment ions m/z (% abundance)[a]			
n=	X=	$[DnPC_2 + X - Me_3N]^+$	$[DnPC + Me]^+$	$[DnPC + X]^+$	other ions[b]
5	H	792 (3)	440 (9)	426 (100)	609 (6)
5	Na	814 (1)	440 (8)	448 (100)	n/a
5	K	830 (1)	440 (6)	464 (100)	n/a
6	H	848 (3)	468 (12)	454 (100)	637 (9)
6	Na	870 (1)	468 (5)	476 (100)	n/a
6	K	886 (2)	468 (4)	492 (100)	n/a
14	H	1298 (6)	693 (14)	679 (100)	862 (16)
14	Na	1320 (1)	693 (6)	701 (100)	n/a
14	K	1336 (2)	693 (4)	717 (100)	n/a

[a]All spectra were carried out with an isolation window of 3 Th and a activation time of 100ms and a Q value of 0.25 and a CID voltage optimized to give a CID spectrum where the precursor ion is about 20% relative abundance to the base peak.
[b]only ions of a relative abundance > 1% are listed.

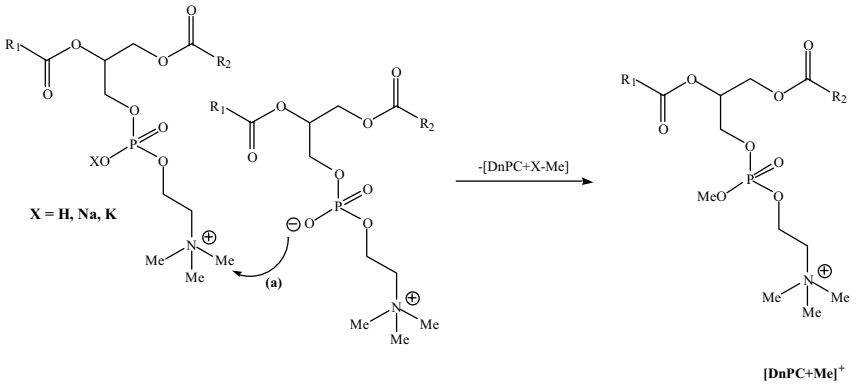

Scheme 2

tramolecular elimination reaction benefits from a 6-membered transition-state.

An important question concerns the issue of whether these intermolecular cluster reactions are unique to CID in a 3D quadrupole ion trap, or if they occur in other types of mass analyzers and under "in-source" CID conditions. To address this issue, we have carried out a series of CID experiments in a linear ion trap (Supplementary Material Figure S4) as well as via "in-source" CID experiments in both the LCQ and the triple quadrupole mass spectrometers. The latter experiments are discussed in the section below.

Similar clusters are observed in the linear ion trap compared to the 3D quadrupole ion trap (Supplementary Material Figure S4A). Under collisionally activated conditions, the protonated dimer fragments via aforementioned pathways. Due to the increased sensitivity of the LTQ, we observe two other peaks, which are attributable to further fragmentation. MS^3 experiments (Supplementary Material Figure S4C-F) support their identities as those proposed earlier and described in further detail below. To further confirm the identity of the charged species and, hence, the neutral loss, similar experiments were carried out with higher mass accuracy on a LTQ-FTMS. Comparison of the masses obtained with the theoretical masses lends support for the elemental compositions of all the proposed species generated via both ESI and CID (Supplementary Material Table S1).

To further probe the formation and structures of the $[D6PC_2 + H - Me_3N]^+$, $[D6PC + Me]^+$, and other product ions, we next examined (1) the role of the charge in their formation by comparing the fragmentation reactions of the related alkali adducts; (2) whether the inter cluster reaction products can be formed via "in-source" CID; and (3) possible structures of the fragmentation reaction products based on a combination of PM3 semi-empirical calculations and MS^3 experiments.

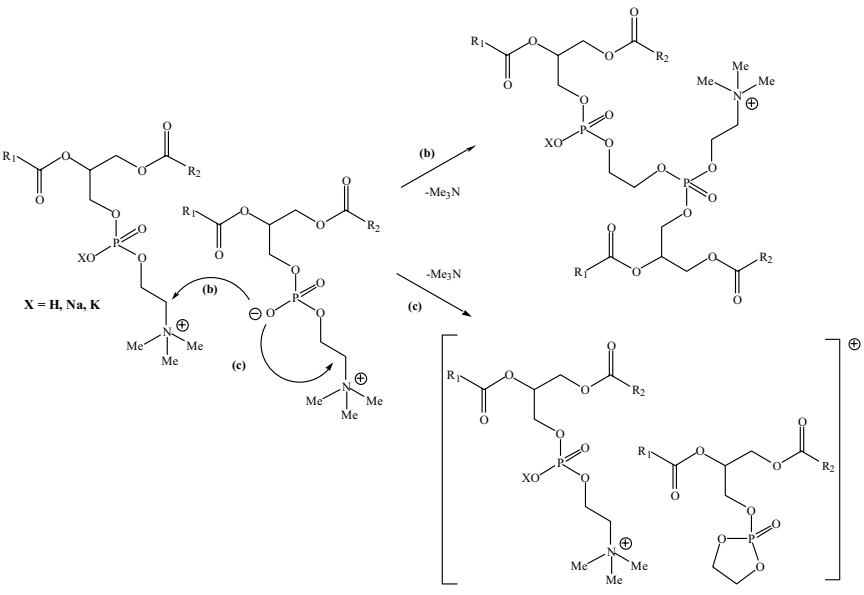

Scheme 3

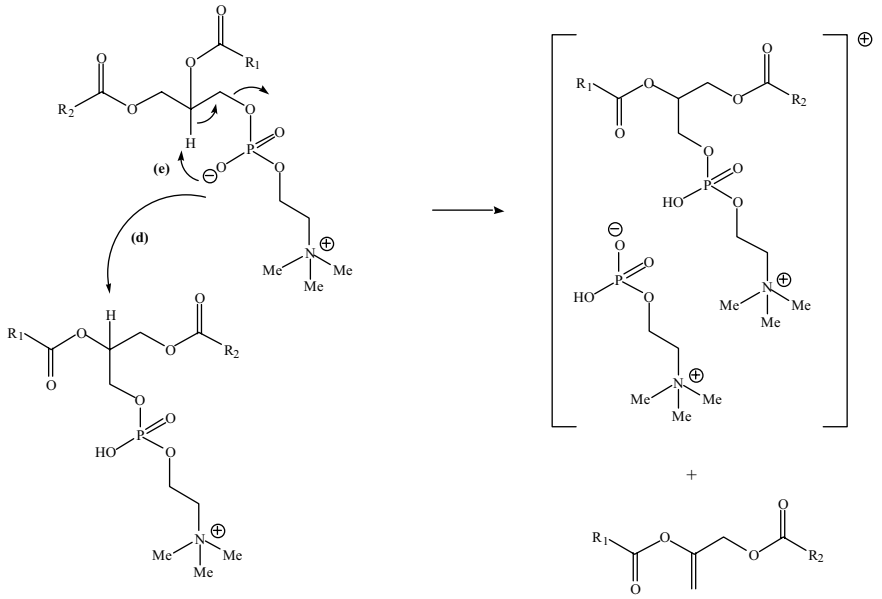

Scheme 4

Role of the Charge in the Formation of the Intercluster CID Products

To gain further insights into the requirements for these intercluster reactions, we have evaluated the role of the charge. This can be changed by either altering the nature of the head group or the cationizing agent. Changing the head group from choline to ethanolamine has a profound effect on the fragmentation of the protonated dimer (Supplementary Material Figure S5). Thus $[D6PE_2 + H]^+$ (*m/z* 823) dissociates to yield the monomer (*m/z* 412) as the dominant product, with only minor amounts of loss of the acyl side-chain occurring [at *m/z* 271 (15%) and at *m/z* 553 (<1%)]. No loss of NH_3 is observed, suggesting that the head group controls whether the intramolecular S_N2 (Path (b) in Scheme **3**) reaction occurs or not.

Altering the cationizing agent also changes the types of reactions observed in the product ion spectra of diacylglycerophosphocholines (Figure 2, where Cat = Na and K). A comparison of the cationized monomers of D6PC reveals that the nature of the charge can have a profound effect on the type of fragmentation reaction that results. Thus when Cat = H, the sole pathway involves formation of the phosphocholine ion at *m/z* 184 (Figure 1d). In contrast, the dominant fragmentation reaction for the alkali earth cationized monomers in-

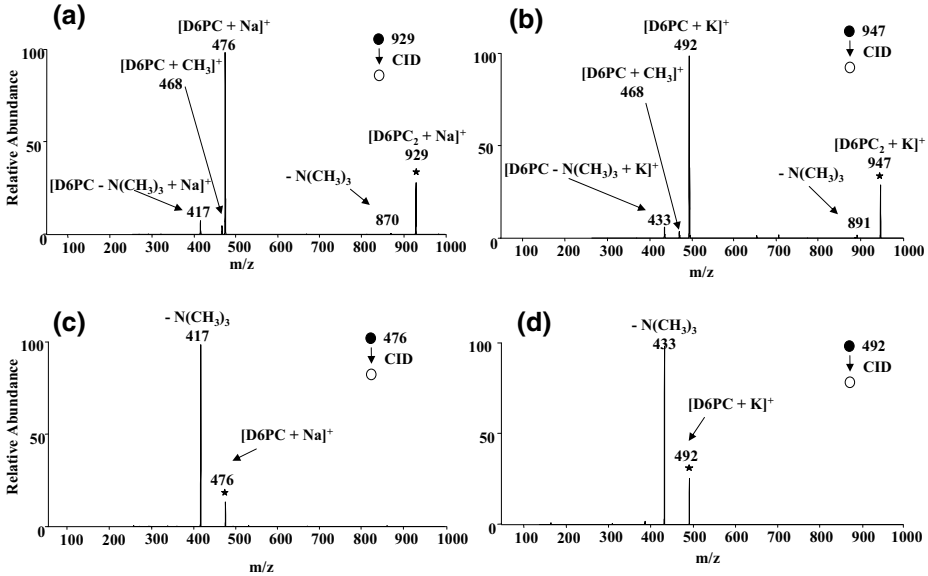

Figure 2. LCQ CID MS/MS of (**a**) $[D6PC_2 + Na]^+$; (**b**) $[D6PC_2 + K]^+$; (**c**) $[D6PC + Na]^+$; (**d**) $[D6PC + K]^+$. The mass selected precursor ion is designated by an asterisk.

volves loss of trimethylamine (Figure 2c and d), consistent with previous studies [20a]. The nature of the charge also plays a role in the fragmentation reactions of the dimers. Not only do the abundances of the intercluster fragmentation reactions significantly diminish in the sodiated and potassiated dimers (Figure 2a and b), but the types of reactions observed also are different. In the case of the protonated dimer cluster, both S_N2 (ions at *m/z* 468 and 848 in Figure 1c) and elimination (ion at *m/z* 637 in Figure 1c) reactions occur. In contrast, the elimination reaction pathway is virtually nonexistent for the sodiated and potassiated dimers (Figure 2a and b). Similar results were found for the D5PC and D14PC homo-dimers (Table 1). While it is not clear why the elimination reaction becomes unfavorable for the alkali earth metal cationized dimers, a possible explanation is that the preference for multidentate coordination by sodium and potassium ions restricts the geometric conformations available for intercluster reactions.

Examination of In-Source Formation of the Intercluster CID Products

Arguably, the biggest concern for the generation of artefacts via intermolecular cluster reactions is their occurrence via "in-source" CID before mass selection. In the LCQ mass spectrometer, the most significant factor controlling in-source CID is the tube lens voltage, while in the triple quadrupole mass spectrometer it is the cone voltage. An examination of the ion signal for the various oligomers as well as the intercluster CID products as a function of the tube lens voltage in the LCQ reveals a complex dependence (Supplementary Material Figure S6). This is because the dimer cluster ion is the source of the intercluster CID products and the dimer ion itself is formed from CID reactions involving the higher oligomeric cluster ions (Figure 1a and b). Nonetheless, the intercluster CID products shown in Schemes **2** and **3** are not only observed at relatively low (typically <50 V) tube lens voltages, but also yield identical product ion spectra to those obtained in MS^3 experiments involving the mass selected protonated dimers (see Supplementary Material Figures S7 and S8). How these product ion spectra relate to the proposed structures of the intercluster CID products are discussed in further detail in another section below.

We have also examined the "in-source" CID reactions in a triple quadrupole mass spectrometer by varying the cone voltage (Supplementary Material Figure S9). At low cone voltage (10 V), the monomer is the predominant species. However, as the cone voltage is increased (100 and 150 V), there is a shift towards the protonated dimer as the predominant species. In addition, higher cone voltages promote the further fragmentation of the protonated dimer to produce some of the species observed earlier under CID conditions. Thus the $[D6PC + Me]^+$ ion (*m/z* 468) and that arising from the elimination pathway (*m/z* 637) are both observed in the spectra at cone voltage of 100 V. In contrast, the "cross-linked" S_N2 reaction product (*m/z* 848) is not observed. This suggests that the source induced dissociation fragmentation conditions in the triple quadrupole are somewhat different from those involved in the formation of the CID products observed in both the quadrupole and linear ion traps.

Possible Structures of the Fragmentation Reaction Products Based on a Combination of PM3 Semi-Empirical Calculations and MS^3 Experiments

How can we confirm the structures of the three key intercluster reaction product ions shown in Schemes **2**, **3**, and **4**? Ideally, this would be achieved by comparing their fragmentation reactions with those of "authentic" ion structures synthesized via other means (i.e., in the condensed or gas phases), or where this is not possible, by examining the types of fragmentation reactions observed and correlating them to related phospholipid fragmentation pathways (including those described in the literature). Here, we focus solely on a detailed discussion of the D6PC product ion structures, although similar results were observed in the product ion spectra of each of the intercluster product ions for the D5PC and D14PC homo-dimers (Table 1).

We were able to unequivocally confirm the identity of the proposed elimination product as being the $[D6PC + PC + H]^+$ complex, since we able to independently "synthesize" an "authentic" structure in the gas phase and show that it yields an essentially identical CID spectrum. This was achieved by combining PC with D6PC in solution and subjecting the resultant mixture to ESI/MS (see Experimental section for details). Although, the $[D6PC + PC + H]^+$ complex was observed in the ESI mass spectrum, to avoid possible contamination of this *m/z* 637 ion from in-source CID reactions of the D6PC homo-dimer, we chose to mass select the hetero-trimer, $[D6PC_2 + PC + H]^+$ [the hetero-trimer, $(D6PC_2 + PC + H)^+$ cannot be contaminated from the homo-trimer of D6PC, as it solely fragments via D6PC loss; see Figure 1b] and subject it to CID, then isolate the resultant $[D6PC + PC + H]^+$ hetero-dimer for subsequent CID studies. MS^3 of this *m/z* 637 produced an identical spectrum (Supplementary Material Figure S10) to the *m/z* 637 intercluster CID product formed from the protonated D6PC dimer. The MS^3 spectrum of the proposed elimination product (Scheme **4**) mainly yields $[D6PC + H]^+$, consistent with it being a noncovalent complex (Supplementary Figure S8). Interestingly, a small amount of the methylated monomer is observed, which may arise via a related intercluster S_N2 reaction (cf Scheme **2**).

Unfortunately, the S_N2 "cross-linked" product ion (formed via Path (b) of Scheme **3**) is a previously unknown species that is not readily synthesized, thus precluding a direct comparison of its CID spectrum.

Nonetheless, an examination of the MS^3 spectrum reveals that the fragmentation reactions are consistent with the "cross-linked" structure, as it fragments via successive cleavages of the two phosphate-glycerol C—O bonds to yield product ions at *m/z* 578 and 308 (Supplementary Material Figure S7A and S7B) rather than via fragmentation to the $[D6PC + H]^+$ monomer, which would be indicative of a noncovalent complex structure for the $[D6PC_2 + H - Me_3N]^+$. Thus, this suggests that the Me_3N loss from the dimer proceeds via Path (b) in Scheme **3** rather than Path (c).

In a similar fashion, the MS^3 spectrum of the proposed S_N2 methylated structure (formed via Scheme **2**) yields methylated phosphocholine at *m/z* 198 (Supplementary Material Figure S7C and S7D), which is analogous to the way that the protonated monomer fragments (Figure 1d) [20a].

While detailed molecular modeling for these systems are beyond the scope of this paper, we were interested in examining the structures and energetics for the products arising from the four fragmentation pathways for the $[D6PC_2 + H]^+$ ions. Unfortunately, these dimers are too large to optimize using high level ab initio or DFT calculations. Simplifying the acyl side-chain to an acetyl group to save on computational expense is not an option since PM3 calculations suggest that this has a profound effect on the structures of these species, as stabilization of conformations via hydrophobic interactions involving the acyl chain are lost (data not shown). Thus, the PM3 level of theory [21] was chosen to optimize these structures using the GAMESS program [22] since it is generally accepted to be the best semi-empirical method for calculating hydrogen bonded structures [23]. Given the size of these systems, a comprehensive search of the conformational space of the reactant and all of the products is beyond the scope of this work. Further complications are that many of these species can be stabilized by a number of different types of electrostatic interactions, and that the proton can reside on a number of different sites. Nonetheless, we include the PM3 calculated structures of the key ionic species arising from the fragmentation of the $[D6PC_2 + H]^+$ dimer in Figure 3, while the energetics for the competition between dissociation to the monomer versus the S_N2 (Scheme **2**, Path (b) of Scheme **3**) and elimination pathways (Scheme **4**) are given in Table 2. [The product of Path (c) in Scheme **3** was not calculated as the MS^3 experiments do not support this structure.] An examination of Figure 3 reveals a number of interesting structural features for each of these ions. In all cases the acyl chains were found to adopt a zigzag conformation and interact with each other via hydrophobic interactions. The phosphocholine head group was found to stabilize conformations by undergoing several different types of electrostatic interactions. Thus, in the protonated monomer, a total of three different conformations were found. In the most stable conformation (Figure 3a), the charged trimethylammo-

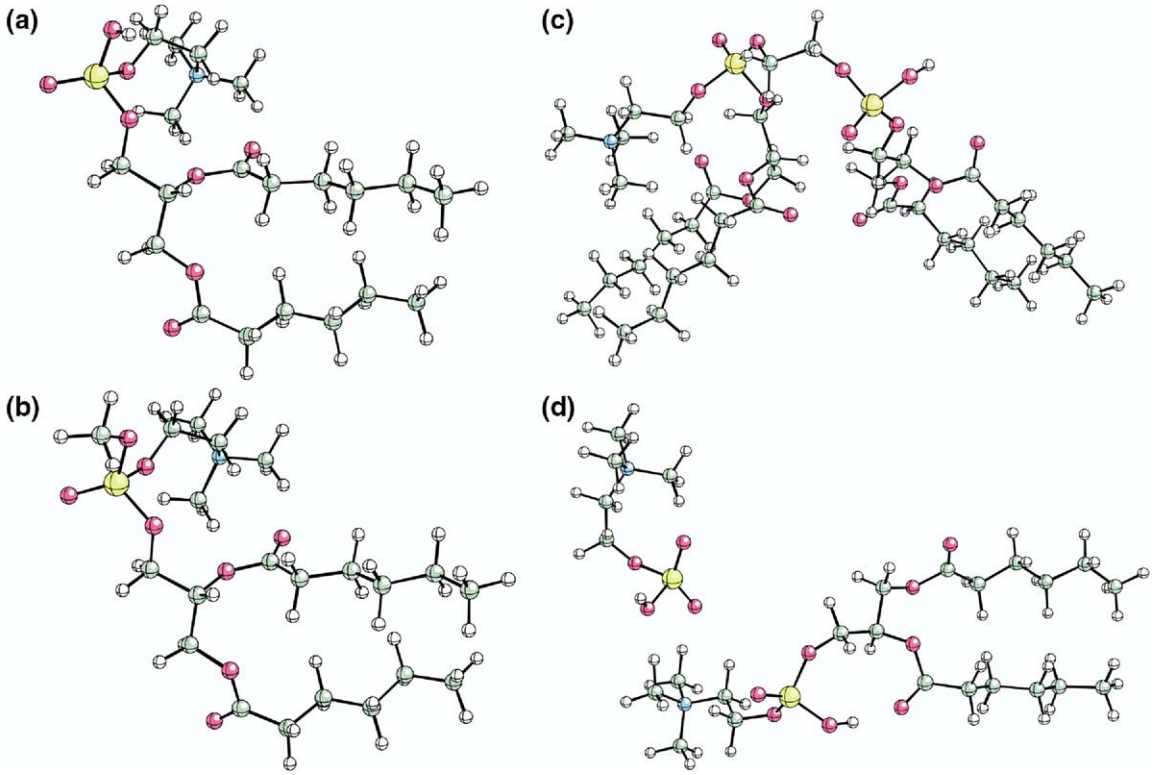

Figure 3. Most stable PM3 calculated structures of: (**a**) $[D6PC_2 + H]^+$; (**b**) $[D6PC + Me]^+$ (formed via Path (a) of Scheme **2**); (**c**) $[D6PC_2 + H - Me_3N]^+$ (formed via Path (b) of Scheme **3**); (**d**) $[D6PC_2 + H - C_{15}H_{26}O_4]^+$ (formed via Scheme **4**).

Table 2. PM3 calculated energetics (in kcal mol^{-1}) for the competition between monomer loss and S_N2 and Elimination reactions for the protonated dimers $[D6PC_2 + H]^+$[a]

Reaction Type	ΔH for $[D6PC_2 + H]^+$	Structure of ion
Monomer loss	25.3	see Figure 3a
S_N2 "cross linking"[b]	−11.8	see Figure 3c
S_N2 methylation[c]	−10.7	see Figure 3b
Elimination[d]	14.5	see Figure 3d

[a]All data are available from the authors upon request.
[b]Yields the products shown in Scheme **2**.
[c]Yields the products shown in Path (b) in Scheme **3**.
[d]Yields the products shown in Scheme **4**.

nium part of the head group interacts with the C=O of one of the acyl chains, while in the remaining conformations the OH of the phosphate interacts with the C=O of one of the acyl chains (data not shown). A total of three conformations of the methylated monomer were found. Interestingly, the most stable conformations of both of the ionic S_N2 products are the ones that exhibit the same type of stabilization by the charged trimethylammonium part of the head group, which interacts with the C=O on one of the acyl chains (Figure 3b and c). The charged elimination product is interesting since it is a protonated dimer in which the proton can reside on either of the phosphate groups. Of the four conformations found, the most stable one has the largest phosphate protonated (Figure 3d).

Although we have not carried out full conformational searches and considered the barrier heights (by calculating the transition states) for these fragmentations reactions, the data in Table 2 reveal some interesting aspects on the thermochemistry associated with these intercluster reactions that are expressed relative to the energy of the starting protonated dimer. Thus, there is an inherent thermodynamic driving force to the S_N2 reactions that are both calculated to be exothermic (Scheme **2** by 11.8 kcal mol^{-1}; Path (b) of Scheme **3** by 10.7 kcal mol^{-1}). In contrast, simple monomer loss and the products from the elimination reactions shown in Scheme **4** are endothermic by 25.3 kcal mol^{-1} and 14.5 kcal mol^{-1}, respectively. In fact, all of the intercluster reactions are thermodynamically favored over simple dissociation to the monomer.

Conclusions

Given the increasing number of studies in biological mass spectrometry, it is surprising that few studies have discussed the issue of artefacts arising in the mass spectra of the common classes of biomolecules. In principle, artefacts may either arise from solution phase reactions or from gas-phase processes. Most studies have focused on understanding rearrangement reactions occurring in the CID spectra of ions derived from monomeric species [24]. It is now becoming apparent that gas-phase intermolecular cluster reactions may also give rise to artefacts.

In the area of lipidomics, the results from this study suggest that three main types of artefacts may be present in ESI mass spectra, and suggest these artefacts may be worth searching for in metabolomic data [15d]. The first class arises from solution phase hydrolyses reactions. Given the large number of samples routinely analyzed, there can often be a significant time delay between collection and analysis of samples. We have shown that significant acid hydrolysis of diacylglycerophospholipids can occur. The second class arises from the formation of lipid cluster ions. Although it has been suggested that the best way of avoiding lipid–lipid interactions in mass spectrometry is to use dilute solutions [15c], the fact that lipid oligomers are observed below their CMC under ESI conditions [14] suggests that these lipid clusters may be formed during the electrospray process via "concentration" of the lipid during the desolvation process. The third class of artefact arises from gas-phase intermolecular cluster reactions. The limited studies reported to date suggest that the structure of the lipid in dimer cluster ions appears to play an important role in the formation of products arising from intermolecular cluster reactions. Simple lithium bound dimers of diacylglycerol appear to be "well behaved", fragmenting to form monomers [25]. In contrast, the phosphate group of phospholipids can be involved in phosphate transfer [2c] or in the S_N2 and elimination reactions described in this work. These latter artefacts may become significant in the detection of minor components in complex lipid mixtures directly infused by ESI/MS, especially where neutral loss strategies are used [19].

Further studies are underway at examining the fundamental gas-phase chemistry of cluster ions of biological relevance, including additional lipid systems.

Acknowledgments

PFJ acknowledges the award of a Heart Foundation Scholarship (Studentship). MAP and RAJO thank the Australian Research Council for financial support. The authors thank the trustees of the A. E. Rowden White foundation for funds to purchase the Thermo Finnegan LCQ DECA mass spectrometer. An ARC LIEF grant and funding from the Victorian Institute for Chemical Sciences is acknowledged for the purchase of the LTQ-FTMS. The authors thank Ms. Sioe See Volaric and Dr. George Khairallah for their assistance in the analysis of samples on the Micromass Triple Quadrupole mass spectrometer. They also thank the referees for their useful comments and suggestions.

References

1. (a) Cooks, R. G., Patrick, J. S., Kotiaho, T., McLuckey, S. A. Thermochemical Determinations by the Kinetic Method. *Mass Spectrom. Rev.* **1994,** *13,* 287; (b) Cooks, R. G.; Koskinen, J. T.; Thomas, P. D. The Kinetic Method of Making Thermochemical Determinations. *J. Mass Spectrom.* **1999,** *34,* 85.
2. (a) Strittmatter, E. F.; Schnier, P. D.; Klassen, J. S.; Williams, E. R. Dissociation Energies of Deoxyribose Nucleotide Dimer Anions Measured Using Blackbody Infrared Radiative Dissociation. *J. Am. Soc. Mass Spectrom.* **1999,** *10,* 1095; (b) Vrkic, A. K.; O'Hair, R. A. J. Gas Phase Reactions of Trimethylborate with the $[M - H]^-$ Ions of Nucleotides and Their Noncovalent Homo- and Heterodimer Complexes. *Aust. J. Chem.* **2003,** *56,* 389; (c) Thomas M. C.; Mitchell, T. W.; Blanksby, S. J.

A Comparison of the Gas Phase Acidities of Phospholipid Headgroups: Experimental and Computational Studies. *J. Am. Soc. Mass Spectrom.* **2005,** *16,* 926.
3. Julian, R. R.; Beauchamp, J. L. Abiotic Synthesis of ATP from AMP in the Gas Phase: Implications for the Origin of Biologically Important Molecules from Small Molecular Clusters. *Int. J. Mass Spectrom.* **2003,** *227,* 147.
4. Cox, H. A.; Hodyss, R.; Beauchamp, J. L. Cluster-Phase Reactions: Gas-Phase Phosphorylation of Peptides and Model Compounds with Triphosphate Anions. *J. Am. Chem. Soc.* **2005,** *127,* 4084–4090.
5. Vrkic, A. K.; O'Hair, R. A. J. Using Noncovalent Complexes to Direct the Fragmentation of Glycosidic Bonds in the Gas Phase. *J. Am. Soc. Mass Spectrom.* **2004,** *15,* 716–725.
6. Gross D. S.; Williams, E. R. On the Dissociation and Conformation of Gas-Phase Methonium Ions. *Int. J. Mass Spectrom. Ion Processes* **1996,** *158,* 305–318.
7. (a) Gronert, S.; Azebu, J. Reactions of Gas-Phase Salts: Substitutions and Eliminations in Complexes Containing a Dianion and a Tetraalklylammonium Cation. *Org. Lett.* **1999,** *1,* 503–596; (b) Gronert, S.; Fong, L.-M. Structural Effects on the Gas-Phase Reactivity of Organic Salt Complexes: Substitution versus Hofmann Elimination. *Aust. J. Chem.* **2003,** *56,* 379–383; (c) Gronert, S. Gas-Phase Studies of the Competition Between Substitution and Elimination Reactions. *Acc. Chem. Res.* **2003,** *36,* 848–857.
8. Waters, T.; O'Hair, R. A. J.; Wedd, A. G. Catalytic Gas-Phase Oxidation of Methanol to Formaldehyde. *J. Am. Chem. Soc.* **2003,** *125,* 3384–3396.
9. Gronert, S.; Fagin, A. E.; Okamoto, K. Stereoselectivity in the Collision-Activated Reactions of Gas Phase Salt Complexes. *J. Am. Soc. Mass Spectrom.* **2004,** *15,* 1509–1516.
10. Hodyss, R.; Cox, H. A.; Beauchamp, J. L. Cluster Phase Reactions: Alkylation of Triphosphate and DNA Anions with Alkylammonium Cations. *J. Phys. Chem. A* **2004,** *108,* 10030–10034.
11. Harrison, K. A.; Murphy, R. C. Negative Electrospray Ionization of Glycerophosphocholine Lipids: Formation of $[M - 15]^-$ ions occurs via collisional decomposition of adduct anions. *J. Mass Spectrom.* **1995,** *30,* 1772–1773.
12. (a) Perugini, M. A.; Schuck, P.; Howlett, G. J. Differences in the Binding Capacity of Human Apolipoprotein E3 and E4 to Size-Fractionated Lipid Emulsions. *Eur. J. Biochem.* **2002,** *269,* 5939–5949; (b) Perugini, M. A.; Schuck, P.; Howlett, G. J. Self-Association of Human Apolipoprotein E3 and E4 in the Presence and Absence of Phospholipid. *J. Biol. Chem.* **2000,** *275,* 36758–36765.
13. Hanson, C. L.; Ilag, L. L.; Malo, J.; Hatters, D. M.; Howlett, G. J.; Robinson, C. V. Phospholipid Complexation and Association with Apolipoprotein C-II: Insights from Mass Spectrometry. *Biophys. J.* **2003,** *85,* 3802–3812.
14. (a) Siuzdak, G., Bothner, B. Gas-Phase Micelles. *Angew. Chem. Int. Ed.* **1995,** *34,* 2053–2055; (b) Cacace, F.; De Petris, G.; Giglio, E.; Punzo, F.; Troiani, A. Bile Salt Aggregates in the Gas Phase: An Electrospray Ionization Mass Spectrometric Study. *Chem. Eur. J.* **2002,** *8,* 1925–1933.
15. (a) Murphy, R. C.; Fiedler, J.; Hevko, J. Analysis of Nonvolatile Lipids by Mass Spectrometry. *Chem. Rev.* **2001,** *101,* 479–526; (b) Pulfer, M.; Murphy, R. C. Electrospray Mass Spectrometry of Phospholipids. *Mass Spectrom. Rev.* **2003,** *22,* 332–364; (c) Han, X. L.; Gross R. W. Shotgun Lipidomics: Electrospray Ionization Mass Spectrometric Analysis and Quantitation of Cellular Lipidomes Directly from Crude Extracts of Biological Samples. *Mass Spectrom. Rev.* **2005,** *24,* 367–412; (d) Forrester, J. S.; Milne, S. B.; Ivanova, P. T.; Brown, H. A. Computational Lipidomics: A Multiplexed Analysis of Dynamic Changes in Membrane Lipid Composition During Signal Transduction. *Mol. Pharmacol.* **2004,** *65,* 813–821.
16. (a) Heerklotz, H.; Epand, R. M. The Enthalpy of Acyl Chain Packing and the Apparent Water-Accessible Apolar Surface Areas of Phospholipids. *Biophys. J.* **2001,** *80,* 271–279; (b) Johnson, R. E.; Wells, M. A.; Rupley, J. A. Thermodynamics of Dihexanoylphospatidylcholine Aggregation. *Biochem.* **1981,** *20,* 4229–4242.
17. Arnhold, J.; Osipov, A. N.; Spalteholz, H.; Panasenko, O. M.; Schiller, J. Formation of Lysophospholipids from Unsaturated Phosphatidylcholines Under the Influence of Hypochlorous Acid. *Biochim. Biophys. Acta* **2002,** *1572,* 91–100.
18. Ilag, L. L.; Ubarretxena-Belandia, I.; Tate, C. G.; Robinson, C. V. Drug Binding Revealed by Tandem Mass Spectrometry of a Protein-Micelle Complex. *J. Am. Chem. Soc.* **2004,** *126,* 14362–14363.
19. Hsu, F.-F.; Turk, J. Charge-Driven Fragmentation Processes in Diacylglycerophosphatidic Acid Upon Low-Energy Collision Activation. A Mechanistic Proposal. *J. Am. Soc. Mass Spectrom.* **2000,** *11,* 797–803.
20. (a) Hsu, F.-F.; Turk, J. Electrospray Ionization/Tandem Quadrupole Mass Spectrometric Studies on Phosphatidylcholines: The Fragmentation Processes. *J. Am. Soc. Mass Spectrom.* **2003,** *14,* 352–363; (b) Hsu, F.-F.; Turk, J.; Thukkani, A. K.; Messner, M. C.; Wildsmith, K. R.; Ford, D. A. Characterization of Alkylacyl, Alk-1-Enylacyl, and Lyso Subclasses of Glycerophosphocholine by Tandem Quadrupole Mass Spectrometry with Electrospray Ionization *J. Mass Spectrom.* **2003,** *38,* 752–763.
21. Stewart, J. J. P. Optimization of Parameters for Semiempirical Methods. 1. Method. *J. Comput. Chem.* **1989,** *10,* 209–220.
22. PC GAMESS version 6.4, build number 2606. Schmidt, M. W.; Baldridge, K. K.; Boatz, J. A.; Elbert, S. T.; Gordon, M. S.; Jensen, J. H.; Koseki, S.; Matsunaga, N.; Nguyen, K. A.; Su, S. J.; Windus, T. L.; DuPuis, M.; Montgomery, J. A. General Atomic and Molecular Electronic Structure System. *J. Comput. Chem.* **1993,** *14,* 1347–1363.
23. (a) Kallies, B.; Mitzner, R. The Ability of the Semiempirical PM3 Method to Model Proton Transfer Reactions in Symmetric Hydrogen Bonded Systems. *J. Mol. Model* **1995,** *1,* 68–78; (b) Denisov, E. V.; Shustryakov, V.; Nikolaev, E. N.; Winkler, F. J.; Medina, R. FT ICR Investigations of Chiral Supramolecular Propellers of Dialkyltartrate Trimers with Methylammonium ions. *Int. J. Mass Spectrom. Ion Processes* **1997,** *167/168,* 259–268.
24. Farrugia, J. M.; O'Hair, R. A. J. Argine Involvement of Salt Bridges in a Novel Gas Phase Rearrangement of Protonated Containing Dipeptides which Precedes Fragmentation. *Int. J. Mass Spectrom.* **2003,** *222,* 229–242 and references cited therein.
25. Ham, B. M.; Cole R. B. Determination of Bond Dissociation Energies Using Electrospray Tandem Mass Spectrometry and a Derived Effective Reaction Path Length Approach. *Anal. Chem.* **2005,** *77,* 4148–4159.